Inorg. Chem. **2009**, *48*, 3667−3678

Proton-Transfer and H_2-Elimination Reactions of Trimethylamine Alane: Role of Dihydrogen Bonding and Lewis Acid−Base Interactions

Oleg A. Filippov,[†] Victoria N. Tsupreva,[†] Lyudmila M. Golubinskaya,[†] Antonina I. Krylova,[†] Vladimir I. Bregadze,[†] Agusti Lledos,*[,‡] Lina M. Epstein,[†] and Elena S. Shubina*[,†]

A. N. Nesmeyanov Institute of Organoelement Compounds, Russian Academy of Sciences, Vavilov Street 28, 119991 Moscow, Russia, and Departament de Química, Edifici Cn, Universitat Autónoma de Barcelona, 08193 Bellaterra, Spain

Received November 25, 2008

Proton-transfer and H_2-elimination reactions of aluminum hydride $AlH_3(NMe_3)$ (TMAA) with XH acids were studied by means of IR and NMR spectroscopy and DFT calculations. The dihydrogen-bonded (DHB) intermediates in the interaction of the TMAA with XH acids (CH_3OH, ^iPrOH, CF_3CH_2OH, adamantyl acetylene, indole, 2,3,4,5,6-pentafluoroaniline, and 2,3,5,6-tetrachloroaniline) were examined experimentally at low temperatures, and the spectroscopic characteristics, dihydrogen bond strength and structures, and the electronic and energetic characteristics of these complexes were determined by combining experimental and theoretical approaches. The possibility of two different types of DHB complexes with polydentate proton donors (typical monodentate and bidentate coordination with the formation of a symmetrical chelate structure) was shown by DFT calculations and was experimentally proven in solution. The DHB complexes are intermediates of proton-transfer and H_2-elimination reactions. The extent of this reaction is very dependent on the acid strength and temperature. With temperature increases the elimination of H_2 was observed for OH and NH acids, yielding the reaction products with Al−O and Al−N bonds. The reaction mechanism was computationally studied. Besides the DHB pathway for proton transfer, another pathway starting from a Lewis complex was discovered. Preference for one of the pathways is related to the acid strength and the nucleophilicity of the proton donor. As a consequence of the dual Lewis acid−base nature of neutral aluminum hydride, participation of a second ROH molecule acting as a bifunctional catalyst forming a six-member cycle connecting aluminum and hydride sites notably reduces the reaction barrier. This mechanism could operate for proton transfer from weak OH acids to TMAA in the presence of an excess of proton donor.

Introduction

In recent years, the interest in main-group metal hydride chemistry has significantly enlarged. Some of these hydrides hold promise as the means of storing hydrogen, for electrochemical applications, e.g., in fuel cells or for electroplating of metals, as possible fuels, and as reducing agents for a wide range of substrates.[1] Protonation of transition-metal hydrides has been widely employed as one of the most common and convenient methods of preparation of dihydrogen complexes.[2] Hydrogen can also be produced from main-group hydrides. Borohydrides of alkaline metals, such as $LiBH_4$, readily evolve hydrogen by hydrolysis,[3,4] and hydrogen elimination from $LiBH_4$ complexes with less-reactive proton donors, such as alcohols, has been reported.[5] However, in contrast to transition-metal hydrides,[6,7] the

* To whom correspondence should be addressed: E-mail: shu@ineos.ac.ru (E.S.S.); agusti@klingon.uab.es (A.L.). Fax: +7 495 1355085 (E.S.S.); +34 93 5812920 (A.L.).
† Russian Academy of Sciences.
‡ Universitat Autónoma de Barcelona.

(1) (a) Aldridge, S.; Downs, S. *Chem. Rev.* **2001**, *101*, 3305–3365. (b) Downs, A. J.; Greene, T. M. *Adv. Inorg. Chem.* **1999**, *46*, 101–171.
(2) (a) Kubas, G. J. *Metal Dihydrogen and σ-Bond Complexes*; Kluwer Academic/Plenum Publishers: New York, 2001. (b) Kubas, G. J. *Chem. Rev.* **2007**, *107*, 4152–4205.
(3) Kojima, Y.; Kawai, Y.; Kimbara, M.; Nakanishi, H.; Matsumoto, S. *Int. J. Hydrogen Energy* **2004**, *29*, 1213–1217.
(4) Filinchuk, Y.; Hagemann, H. *Eur. J. Inorg. Chem.* **2008**, 3127–3133.
(5) (a) Custelcean, R.; Jackson, J. E. *J. Am. Chem. Soc.* **1998**, *120*, 12935–12941. (b) Custelcean, R.; Jackson, J. E. *J. Am. Chem. Soc.* **2000**, *122*, 5251–5257. (c) Custelcean, R.; Vlassa, M.; Jackson, J. E. *Angew. Chem., Int. Ed.* **2000**, *39*, 3299–3302.
(6) (a) Belkova, N. V.; Shubina, E. S.; Epstein, L. M. *Acc. Chem. Res.* **2005**, *38*, 624–631. (b) Belkova, N. V.; Epstein, L. M.; Shubina, E. S. *ARKIVOC* **2008**, (iv), 120–138.

10.1021/ic802262h CCC: $40.75
Published on Web 03/12/2009

mechanism of proton-transfer reactions to main-group hydrides has been much less explored. Discovery of dihydrogen-bonded (DHB) complexes[8,9] formed by main-group hydrides led to a new perspective on H_2-elimination processes.[10] The ability of main-group hydrides to form dihydrogen bonds was initially studied by experimental and theoretical methods for boron hydrides.[11,12] Theoretical investigations showed the formation of weak dihydrogen bonds by neutral BH_3NEt_3 and BH_3OEt_3 hydrides and the strong base behavior of ionic BH_4^- hydride.[12b] Theoretical studies of the dihydrogen bond between simple main-group hydrides and proton donors (for example, LiH, BeH_2, MgH_2, BH_3, and AlH_3 with HF, H_2O, and NH_3) as models to elucidate the H···H interaction nature have also been published.[13−15]

Experimental detection of EH···HX (E = Al and Ga) interactions in solution is still scarce. Recently variable-temperature IR investigations of the DHB adduct formed between GaH_4^- and weak XH acids in combination with theoretical study were reported by our group.[16] The chemistry of aluminum hydrides has been the subject of numerous experimental and theoretical studies in diverse areas ranging from synthetic chemistry[17] to film growth of aluminum-containing materials.[18] Despite the wide use of aluminum hydrides, little is known about the mechanism by which they react. The structures and decomposition paths of DHB complexes between AlH_4^- and three proton donors (H_2O, HF, and HCl) were studied by ab initio methods.[19] However, the large reaction activity of aluminum tetrahydride makes it difficult to study the DHB formation and proton transfer experimentally in solution. The tetramethylpiperidine adduct of alane features a weak Al−H···H−N dihydrogen bond in the solid state, and it was suggested that this interaction represents a transition state for dihydrogen elimination.[20] The selective reaction at the bridging hydride of pyrazolate- and hydride-bridged dialuminum complexes with protic acids[21] was theoretically explained as resulting from Al−H···H−O dihydrogen bonding.[21,22] We performed a computational study of proton-transfer and H_2-elimination reactions of group 13 hydrides EH_4^- (E = B, Al, and Ga) with alcohols.[23] The general features of the reaction mechanism were deduced from this study: the DHB adduct (EH···HO) initially formed leads, after overcoming the activation barrier, to the concerted step of H_2-elimination and alkoxo product formation. A comparison was made with the mechanism of the proton-transfer reaction to transition-metal hydrides. The energy barrier for AlH_4^- alcoholysis was found to be the lowest in the group, in agreement with the high reactivity of alumohydrides in protic media.

We anticipate the decreased reactivity of a neutral aluminum hydride should allow a deeper experimental study of dihydrogen bond formation with proton donors in solution. Here we will present the results of the spectroscopic and theoretical investigation of the neutral trimethylamine alane ($AlH_3(NMe_3)$, TMAA, and **1**). We have the aim to demonstrate the interaction of **1** with a large series of XH (X = O, N, and C) acids and to elucidate the peculiarities of the mechanism of proton-transfer and H_2- elimination reactions of **1** with different mono- and polydentate acids.

Experimental Section

Experimental Details. Trimethylamine alane, $Me_3N\cdot AlH_3$, was obtained according to ref 24 by a preliminary preparation of an ether−toluene solution of aluminum hydride. $AlCl_3$ (3.33 g, 25 mmol) in ether was added to a suspension of $NaAlH_4$ (4.6 g, 85 mmol) in 700 mL of ether−toluene mixture (1:3) in 30 min, and the mixture was stirred for 4 h. $NaAlH_4$ was additionally milled in a vibration mill filled with steel balls. NaCl precipitate was filtrated,

(7) (a) Bakhmutov, V. I. *Eur. J. Inorg. Chem.* **2005**, 245–255. (b) Besora, M.; Lledós, A.; Maseras, F. *Chem. Soc. Rev.*, **2009**, DOI:10.1039/B608404B.
(8) Crabtree, R. H.; Siegbahn, P. E. M.; Eisenstein, O.; Rheingold, A. L.; Koetzle, T. F. *Acc. Chem. Res.* **1996**, *29*, 348–354.
(9) Bakhmutov, V. I. *Dihydrogen Bonds: Principles, Experiments, and Applications*; John Wiley & Sons, Inc.: Hoboken, NJ, 2008.
(10) Kenward, A. L.; Piers, W. E. *Angew. Chem., Int. Ed.* **2008**, *47*, 38–41.
(11) Richardson, T. B.; de Gala, S.; Crabtree, R. H.; Siegbahn, P. E. M. *J. Am. Chem. Soc.* **1995**, *117*, 12875–12876.
(12) (a) Shubina, E. S.; Bakhmutova, E. V.; Saitkulova, L. N.; Epstein, L M. *Mendeleev Commun.* **1997**, 83–84. (b) Epstein, L. M.; Shubina, E. S.; Bakhmutova, E. V.; Saitkulova, L. N.; Bakhmutov, V. I.; Gambaryan, N. P.; Chistyakov, A. L.; Stankevich, I. V. *Inorg. Chem.* **1998**, *37*, 3013–3017. (c) Shubina, E. S.; Belkova, N. V.; Bakhmutova, E. V.; Saitkulova, L. N.; Ionidis, A. V.; Epstein, L. M. *Russ. Chem. Bull.* **1998**, *47*, 846–851.
(13) Cybulski, H.; Pecul, M.; Sadlej, J. *J. Chem. Phys.* **2003**, *119*, 5094–5104.
(14) (a) Kulkarni, S. A. *J. Phys. Chem. A* **1998**, *102*, 7704–7711. (b) Kulkarni, S. A.; Srivastava, A. K. *J. Phys. Chem. A* **1999**, *103*, 2836–2842. (c) Kulkarni, S. A. *J. Phys. Chem. A* **1999**, *103*, 9330–9335. (d) Cramer, C. J.; Gladfelter, W. L. *Inorg. Chem.* **1997**, *36*, 5358–5362.
(15) (a) Alkorta, I.; Elguero, J.; Mo, O.; Yañez, M.; Del Bene, J. *J. Phys. Chem. A* **2002**, *106*, 9325–9330. (b) Grabowski, S. J.; Sokalski, W. A.; Leszczynski, J. *J. Phys. Chem. A* **2004**, *108*, 5823–5830. (c) Grabowski, S. J.; Sokalski, W. A.; Leszczynski, J. *J. Phys. Chem. A* **2005**, *109*, 4331–4341.
(16) Belkova, N. V.; Filippov, O. A.; Filin, A. M.; Teplitskaya, L. N.; Shmyrova, Y. V.; Gavrilenko, V. V.; Golubinskaya, L. M.; Bregadze, V. I.; Epstein, L. M.; Shubina, E. S. *Eur. J. Inorg. Chem.* **2004**, 3453–3461.
(17) (a) Paquette, L. A. In *Encyclopedia of Reagents for Organic Synthesis*; Paquette, L. A., Ed.; Wiley: Chichester, U.K., 1995, vol 5, pp 3009−3014. (b) Galatsis, P. In *Encyclopedia of Reagents for Organic Synthesis*; Paquette, L. A., Ed.; Wiley: Chichester, U.K., 1995, vol 3, pp 1908−1912. (c) Seyden-Penne, J. *Reductions by the Alumino- and Borohydrides in Organic Synthesis*; VCH: New York, 1991. (d) Eisch, J. J. In *Comprehensive Organic Synthesis*; Trost, B. M., Fleming, I., Eds.; Pergamon: Oxford, U.K., 1991, vol 8, pp 733−761. (e) Zweifel, G.; Miller, J. A. In *Organic Reactions*; Dauben, W. G., Ed.; Wiley: New York, 1984, vol 32, pp 375−517. (f) Hajos, A. *Complex Hydrides and Related Reducing Agents in Organic Synthesis*; Elsevier: New York, 1979.
(18) (a) Jang, T. W.; Rhee, H. S.; Ahn, B. T. *J. Vac. Sci. Technol., A* **1999**, *17*, 1031–1035. (b) Jang, T. W.; Moon, W.; Baek, J. T.; Ahn, B. T. *Thin Solid Films* **1998**, *333*, 137–141. (c) Choi, H.; Hwang, S. *Chem. Mater.* **1998**, *10*, 2323–2325. (d) Yun, J. H.; Kim, B. Y.; Rhee, S. W. *Thin Solid Films* **1998**, *312*, 259–263.
(19) Marincean, S.; Jackson, J. E. *J. Phys. Chem. A* **2004**, *108*, 5521–5526.
(20) Atwood, J. L.; Koutsantonis, G. A.; Lee, F.-C.; Raston, C. L. *J. Chem. Soc., Chem. Commun.* **1994**, 91–92.
(21) Yu, Z.; Wittbrodt, J. M.; Xia, A.; Heeg, J.; Schlegel, H. B.; Winter, C. H. *Organometallics* **2001**, *20*, 4301–4303.
(22) Shi, F.-Q.; Song, B.-A. *Int. J. Quantum Chem.* **2008**, *108*, 1107–1113.
(23) Filippov, O. A.; Filin, A. M.; Belkova, N. V.; Tsupeva, V. N.; Lledós, A.; Ujaque, G.; Epstein, L. M.; Shubina, E. S. *Inorg. Chem.* **2006**, *45*, 3086–3096.
(24) Zakharkin, L. I.; Gavrilenko, V. V.; Maslin, D. N. *Russ. J. Gen. Chem.* **1971**, *41*, 577.

and the solution was cooled to 0 °C. Me_3N (5.9 g, 100 mmol) was added to an ether−toluene solution of AlH_3. After removing the solvent, a powder of trimethylamine alane (8.2 g, yield 92%, mp 74−75 °C) was obtained.

Fluorinated alcohols were provided by P&M (Moscow, Russia). The solutions for IR studies were prepared under argon by standard Schlenk technique. Hexane and methylcyclopentane (Sigma-Aldrich) were purified by distillation from CaH_2 before use. The anhydrous solvents were thoroughly degassed prior to use. The IR spectra of hexane and methylcyclopentane solutions were measured by an Infralum FT-801 (Lumex) FTIR spectrometer. Low-temperature IR studies were carried out in the ν(OH) (3700−3100 cm^{-1}) and ν(AlH) (1950−1600 cm^{-1}) regions by use of a home-modified cryostat (Carl Zeiss Jena) in the 140−300 K temperature range. The cryostat modification allows the transfer of the reagents (premixed either at low or room temperature) directly into the cell under an inert atmosphere and at the desired temperature. The accuracy of the temperature adjustment was ±0.5 K. For the measurements in the ν(XH) range, the XH acid concentrations were 10^{-2} to 10^{-3} M to avoid self-association, whereas TMAA was taken in excess (from 1.2- to 3-fold). For the measurements in the ν(AlH) range, the 1.5- to 4-fold excess of XH acids was used.

Room-temperature NMR spectra were measured on a Bruker AVANCE 600 spectrometer. The ^1H chemical shifts were calculated from the resonances of toluene-d_8 as the internal standard. The ^{27}Al NMR spectra were measured using a 1 M solution of $AlCl_3$ in water as the external standard. The studied solutions were prepared in cold toluene-d_8 and were transferred into NMR tubes. The concentrations of both compounds were taken the same as in the case of the IR investigations.

Computational Details. We have employed the same methodology we successfully applied earlier for the study of DHB complexes of anionic group 13 tetrahydrides.[23] Full geometry optimizations were carried out with the GAUSSIAN03[25] package at DFT level using the hybrid B3LYP functional.[26] The 6-311++G(d,p) basis set was used for all the atoms. The nature of all the stationary points on the potential energy surfaces was confirmed by a vibrational analysis. IRC calculations were carried out in both directions starting from the located transition states. Natural atomic charges and Wiberg bond indices[27] were calculated using the natural-bond orbital (NBO) analysis[28] option as incorporated in GAUSSIAN03. Topological analysis of the electron-density distribution function $\rho(r)$ was performed using the AIMPAC program package[29] based on the wave function obtained by the B3LYP calculations.

Table 1. Spectroscopic Characteristics of DHB Complexes of Monodentate Proton Donors with $AlH_3(NMe_3)$ in Hexane and MCP

HX	$\nu(XH)^{init}$, cm^{-1}	$\nu(XH)^{bond}$, cm^{-1}	$\Delta(XH)$,[a] cm^{-1}
indole	3496	3278	214
AdCCH	3312	3249	63
^{i}PrOH	3604	3392	212

[a] $\Delta(XH) = \nu(XH)^{init} - \nu(XH)^{bond}$.

Results and Discussion

Characterization of Dihydrogen-Bonded Intermediates. The interaction of $AlH_3(NMe_3)$ **1** with monodentate XH acids (adamantyl acetylene (AdCCH), indole, CH_3OH, $(CH_3)_2CHOH$ (^{i}PrOH), and CF_3CH_2OH (TFE)) and polydentate XH_2 acids (2,3,4,5,6-pentafluoroaniline (PFA) and 2,3,5,6-tetrachloroaniline (TeCA)) was investigated by IR and NMR spectroscopy in solvents of low polarity (hexane and methylcyclopentane) in the temperature range of 140−300 K. DFT calculations were performed to analyze the Al−H···HX interaction.

IR Spectroscopic Investigation with Monodentate CH, NH, and OH Acids. The IR spectra of indole were measured in hexane and methylcyclopentane (MCP) with an excess of aluminum hydride. The intensity of the initial $\nu(NH)^{init}$ = 3496 cm^{-1} band decreases in the presence of TMAA, and a new low-frequency broad band at 3278 cm^{-1} appears (Table 1). This illustrates the formation of a DHB complex between the proton donor and aluminum hydride. The intensities of the $\nu(NH)^{bond}$ bands increase as the temperature decreases. In the IR spectra of AdCCH in MCP, the initial band is observed at 3312 cm^{-1} in the range of CH group stretching vibrations. Addition of 4 equiv of TMAA in the temperature range of 140−220 K decreases the intensity of $\nu(CH)^{init}$, and a new broad band at 3249 cm^{-1} appears, which can be attributed to the formation of AlH···HC dihydrogen bond. The intensity of this new band lowers upon warming, and the band completely disappears already at 240 K.

In the range of the Al−H stretching vibrations of TMAA ($\nu(AlH)^{init}$ = 1704 cm^{-1}), the new low-frequency band $\nu(AlH)^{bond}$ = 1660 cm^{-1} (as overlapping broad shoulder, $\Delta\nu(AlH)$ = 44 cm^{-1}) appears at 140 K in the presence of AdCCH (Figure 1). The intensity of $\nu(AlH)^{bond}$ band lowers upon warming, disappearing completely at 240 K. It was shown earlier that dihydrogen bond formation results in a low-frequency shift of the M−H or B−H and Ga−H stretching frequencies for the groups participating in H-bonding.[12b,30] Thus, the spectral changes observed for the TMAA−AdCCH system correspond to formation of AlH···HC DHB complex.

In the case of indole, when the temperature increases, high-frequency shoulders (1754 and 1784 cm^{-1}) appear in the

(25) Frisch, M. J. ; Trucks, G. W.; Schlegel, H. B.; Scuseria, G. E.; Robb, M. A.; Cheeseman, J. R.; Montgomery, Jr., J. A.; Vreven, T.; Kudin, K. N.; Burant, J. C.; Millam, J. M.; Iyengar, S. S.; Tomasi, J.; Barone, V.; Mennucci, B.; Cossi, M.; Scalmani, G.; Rega, N.; Petersson, G. A.; Nakatsuji, H.; Hada, M.; Ehara, M.; Toyota, K.; Fukuda, R.; Hasegawa, J.; Ishida, M.; Nakajima, T.; Honda, Y.; Kitao, O.; Nakai, H.; Klene, M.; Li, X.; Knox, J. E.; Hratchian, H. P.; Cross, J. B.; Bakken, V.; Adamo, C.; Jaramillo, J.; Gomperts, R.; Stratmann, R. E.; Yazyev, O.; Austin, A. J.; Cammi, R.; Pomelli, C.; Ochterski, J. W.; Ayala, P. Y.; Morokuma, K.; Voth, G. A.; Salvador, P.; Dannenberg, J. J.; Zakrzewski, V. G.; Dapprich, S.; Daniels, A. D.; Strain, M. C.; Farkas, O.; Malick, D. K.; Rabuck, A. D.; Raghavachari, K.; Foresman, J. B.; Ortiz, J. V.; Cui, Q.; Baboul, A. G.; Clifford, S.; Cioslowski, J.; Stefanov, B. B.; Liu, G.; Liashenko, A.; Piskorz, P.; Komaromi, I.; Martin, R. L.; Fox, D. J.; Keith, T.; Al-Laham, M. A.; Peng, C. Y.; Nanayakkara, A.; Challacombe, M.; Gill, P. M. W.; Johnson, B.; Chen, W.; Wong, M. W.; Gonzalez, C.; Pople, J. A. *Gaussian 03*, Revision C.02; Gaussian, Inc.: Wallingford, CT, 2004.
(26) Becke, A. D. *J. Chem. Phys.* **1993**, *98*, 5648–5652.
(27) Wiberg, K. *Tetrahedron* **1968**, *24*, 1083–1096.
(28) (a) Reed, A. E.; Curtiss, L. A.; Weinhold, F. *Chem. Rev.* **1988**, *88*, 899–926. (b) Glendening, E. D.; Badenhoop, J. K.; Reed, A. E.; Carpenter, J. E.; Bohman, J. A.; Morales, C.; Weindhold, F. *NBO 5.0*, Theoretical Chemistry Institute, University of Wisconsin: Madison, WI, 2001.
(29) Cheeseman, J.; Keith, T. A.; Bader, R. W. F. *AIMPAC program package*, McMaster University: Hamilton, Ontario (Canada), 1992.
(30) Epstein, L. M.; Belkova, N. V.; Shubina, E. S. In *Recent Advances in Hydride Chemistry*; Peruzzini, M., Poli, R., Eds.; Elsevier: Amsterdam, Netherlands, 2001, pp 351−374.

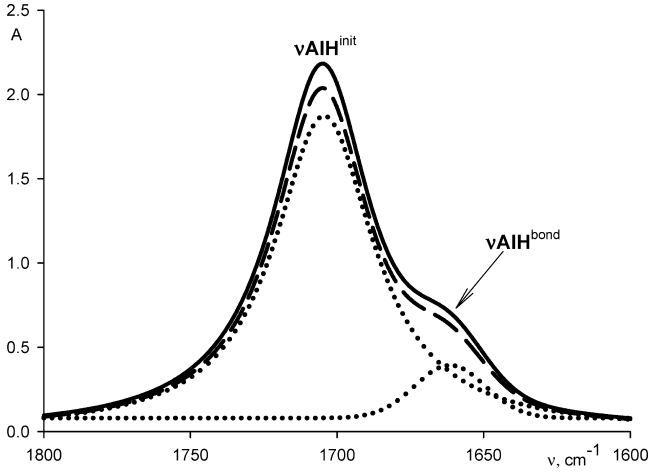

Figure 1. IR spectra in the ν(AlH) range of $AlH_3(NMe_3)$ ($c = 0.03$M) in the presence of 0.09 M AdCCH at 140 K (solid line) and at 160 K (dashed line) with band decomposition (dotted lines), MCP, $d = 0.22$ cm.

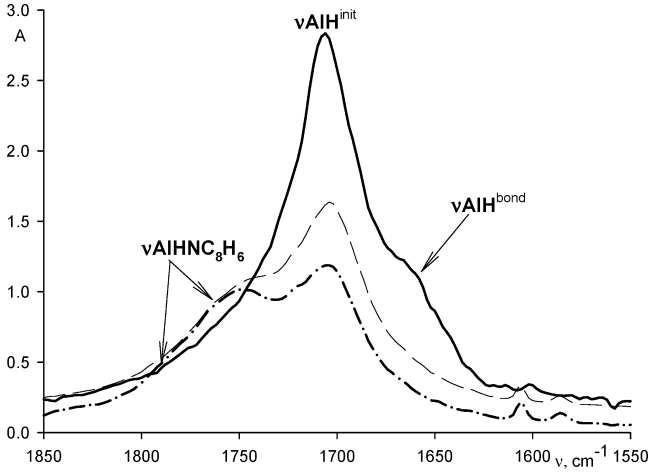

Figure 2. IR spectra in the ν(AlH) range of $AlH_3(NMe_3)$ ($c = 0.03$M) in the presence of 0.06 M indole at 140 K (solid line), at 260 K (dashed line), and at 280 K (dash-dot line), MCP, $d = 0.22$ cm.

Al−H region (Figure 2). It was shown earlier that when one hydrogen of a GaH_4^- is substituted as a result of reaction, the IR spectra of the compounds derived feature three high-frequency bands in the range of the Ga−H stretching vibration,[16] corresponding to GaH_3X^- product. Based on this work, we can assign these two bands to the formation of the monosubstituted product:

$$(Me_3N)AlH_3 + HX \rightleftarrows (Me_3N)H_2AlH\cdot\cdot HX \rightarrow (Me_3N)H_2AlX + H_2 \quad (1)$$

When XH = indole increasing the temperature to 260 K shifts the equilibrium to proton-transfer products. At 290 K, we observe only the reaction product bands (1754 and 1784 cm^{-1}). The interaction between TMAA and AdCCH is weaker and does not result in any further reaction, the equilibrium being displaced toward free reagents upon warming to room temperature.

Structural Analysis. The geometries of TMAA complexes with XH acids were optimized with the DFT method using the B3LYP functional and 6-311++G(d,p) basis set. This methodology was successfully applied earlier by us for DHB complexes of anionic 13 group tetrahydrides.[23] Pyrrole and phenylacetylene were used as models of NH and CH acids, correspondingly, and CH_3OH, CF_3CH_2OH, and CF_3OH were used as models of OH acids of different strength.

Minima corresponding to DHB complexes with CH and NH proton donors were found (Figure 3 and Table 2). Phenylacetylene forms with TMAA a weak DHB complex **1·PHA** with H···H distance of 2.200 Å, only slightly shorter than the sum of hydrogen van der Waals radii (2.4 Å). The interaction is stronger for pyrrole as the H···H distance in **1·Pyrr** (1.870 Å) shows. The changes in the X−H and Al−H bonds after adduct formation are small but typical for dihydrogen bonds, confirming the dihydrogen bond formation.[23] Dihydrogen bond formation entails low-frequency shifts of the ν(XH) and ν(AlH) bands. For example, calculated frequency shifts are $\Delta\nu^{calc}(NH) = 143$ cm^{-1} for the TMAA−pyrrole DHB complex and $\Delta\nu^{calc}(CH) = 61$ cm^{-1} for the TMAA−PhCCH complex. These changes are in good agreement with the experimental data.

Minima on the potential energy surface corresponding to DHB complexes were also found for the TMAA adducts with OH acids: TMAA−CH_3OH **1·M_a,** TMAA−CF_3CH_2OH **1·TFE_a**, and TMAA−CF_3OH **1·TFM_a**. The optimized geometry of a DHB complex with methanol is depicted in Figure 4a. The O−H···H−Al interactions are stronger than those involving C−H or N−H bonds and lead to more pronounced changes in geometries of partners. The structural characteristics obtained (Table 2) are comparable to those observed for related DHB complexes of main-group neutral trihydrides.[12b,14] Increasing of the ROH proton-donating ability in the series $CH_3OH < CF_3CH_2OH < CF_3OH$ results in shortening of the H···H distance and larger elongations of O−H and Al−H bonds involved in the interaction. Comparing DHB complexes of anionic AlH_4^-−ROH[23] with neutral TMAA−ROH, we can observe that H···H bond length is shorter and elongations of O−H and Al−H bonds are larger for the anionic tetrahydride. These structural characteristics of dihydrogen bonds usually are in strong correlation with the proton-accepting ability of hydrides; thus, the lower basicity in the H-bond of TMAA, comparing to the AlH_4^- anion, is similar to what happens in the BH_3NEt_3−BH_4^- pair.[12b]

A second minimum was found for the TMAA−CH_3OH (**1·M_b**) and TMAA−TFE (**1·TFE_b**) complexes. In both systems, it corresponds to the coordination of an oxygen lone pair to the aluminum atom with formation of a Lewis acid−base complex in which aluminum is five-coordinated with a bipyramidal trigonal structure (Figure 4b). The amine and alcohol ligands are occupying the axial positions of the BPT (N−Al−O angle: 176.5° in **1·M_b** and 178.5° in **1·TFE_b**). Formation of the Lewis complex leads to an Al−N bond elongation of 0.063 Å for **1·TFE_b** and 0.106 Å for the stronger **1·M_b** complex, in contrast to the DHB complexes where Al−N bond shortens by 0.005−0.009 Å. A weak H···H interaction is also at work in these Lewis complexes. Despite the fact the H···H distances are larger than the sum of vdW radii of hydrogens and absence of electronic density (Wiberg bond index (WBI), critical points),

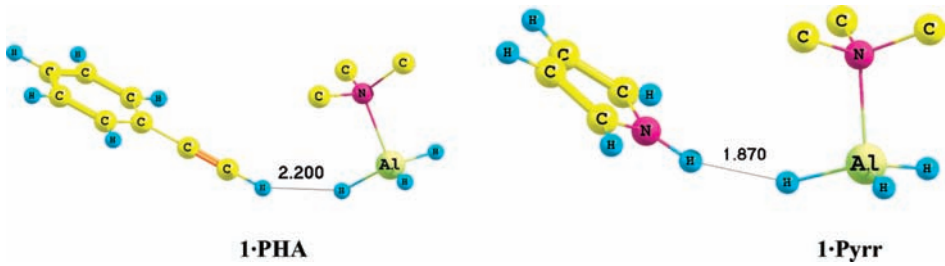

Figure 3. Optimized geometries of complexes of TMAA with phenylacetylene **1·PHA** (left) and pyrrole **1·Pyrr** (right) (hydrogen atoms of NMe_3 removed for clarity).

Table 2. Calculated Selected Structural Parameters (Å and degrees) of TMAA and AlH_4^- Complexes with OH, NH, and CH Proton Donors

complex	rH···H (rAl···O)	∠XH···H	Δr(XH)[a]	Δr(AlH)^{bond}[a]	Δr(AlH)^{free}[a]
TMAA−PhCCH **1·PHA**	2.200	152.4	0.005	0.002	−0.002
TMAA−Pyrrole **1·Pyrr**	1.870	157.9	0.008	0.007	−0.004
TMAA− CH_3OH **1·M_a**	1.702(3.853)	160.5	0.011	0.009	−0.004
AlH_4^-−CH_3OH[b]	*1.622(4.005)*	*164.6*	*0.023*	*0.012*	*−0.009*
TMAA−CH_3OH 1·M_b	**2.581(2.212)**	**81.3**	**0.002**		**0.010**
TMAA−TFE **1·TFE_a**	1.599(3.892)	172.6	0.014	0.014	−0.007
AlH_4^-−TFE[b]	*1.513(3.806)*	*174.8*	*0.027*	*0.017*	*−0.013*
TMAA−TFE 1·TFE_b	**2.775(2.367)**	**76.6**	**0.002**		**0.005**
TMAA−CF_3OH **1·TFM_a**	1.478(3.804)	167.2	0.028	0.016	−0.010
AlH_4^-−CF_3OH[b]	*1.258(3.789)*	*179.2*	*0.086*	*0.030*	*−0.019*

[a] Δr = r(initial) − r(complex). [b] From ref 23.

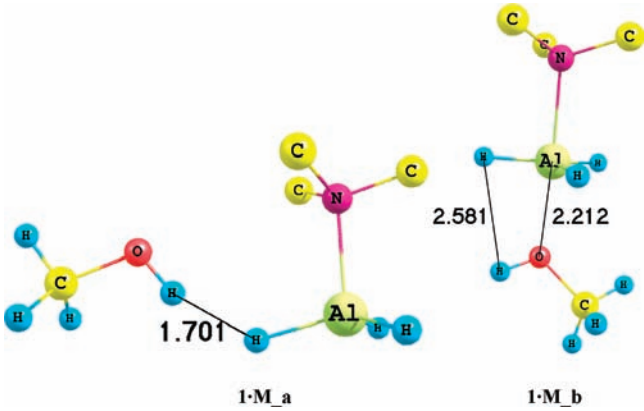

Figure 4. Optimized geometries of TMAA adducts with methanol: DHB complex **1·M_a** (left) and Lewis complex **1·M_b** (right) (hydrogen atoms of NMe_3 removed for clarity).

Table 3. Changes of NPA Charges (Δq), WBI, Electron Densities (ρ_c) at the H···H or Al···O Bond Critical Points, and Complexation Energies for the TMAA and AlH_4^-Complexes with CH, NH, and OH Proton Donors

complex	Δq(Al)	Δq(X)[a]	WBI	ρ_c	ΔE,[d] kcal·mol^{-1}
TMAA−PhCCH	0.023	−0.009	0.005	0.008	−1.4
TMAA−Pyrrole	0.045	−0.014	0.015	0.015	−3.4
TMAA−CH_3OH **1·M_a**	0.053	−0.048	0.025	0.022	−5.6
AlH_4^-−CH_3OH[b]	*0.059*	*−0.055*	*0.047*	*0.026*	*−10.1*
TMAA−CH_3OH 1·M_b[c]	**−0.028**	**0.010**	**0.172**	**0.029**	**−4.8**
TMAA−TFE **1·TFE_a**	0.065	−0.048	0.041	0.027	−5.7
AlH_4^-−TFE[b]	*0.072*	*−0.074*	*0.076*	*0.035*	*−16.0*
TMAA−TFE 1·TFE_b[c]	**−0.034**	**0.015**	**0.132**	**0.021**	**−2.8**
TMAA−CF_3OH **1·TFM_a**	0.087	−0.061	0.071	0.035	−8.2
AlH_4^-−CF_3OH[b]	*0.138*	*−0.049*	*0.191*	*0.063*	*−22.2*

[a] X = C, N for CH, NH, and OH acids. [b] From ref 23. [c] WBI, ρ_c are for Al−O bond. [d] ΔE + ZPVE in kcal·mol^{-1}.

this weak AlH···HO contact results in the very small elongation of the OH bond (∼0.002 Å) in **1·M_b** and **1·TFE_b**. This elongation leads to small low-frequency shifts of ν(OH) (17 and 20 cm^{-1} for **1·M_b** and **1·TFE_b**, respectively) without changes in intensity.

The three ν(AlH) vibrations shift to a low frequency range, but the intensity of these vibrations does not increase. The high-frequency band of ν(AlH)^{free} is absent, in contrast to DHB complexes. Therefore, trends in νAlH vibrations allow distinguishing Lewis and DHB complexes by spectra.

Notably CF_3OH, which is a stronger proton donor (Brønsted acid) but a weaker electron donor (Lewis base), does not form the Lewis complex in a gas phase. Optimizations starting from a Lewis adduct structure always end up in the DHB complex. The evolution of the relative energies of DHB and Lewis complexes agrees with the competition between Brønsted acidity and Lewis basicity of the alcohols. For methanol both complexes (**1·M_a** and **1·M_b**) have similar stabilities, the DHB complex being only 0.8 kcal·mol^{-1} more stable than the Lewis complex (Table 3). This difference considerably increases to 2.9 kcal·mol^{-1} for the trifluoroethanol complexes until disappearance of the Lewis complex for trifluoromethanol.

Electron-Density Analysis. Formation of DHB and Lewis complexes entails transfer of electron density between the two units constituting the complex and rearrangements of density within the confines of the interacting molecules. The electron density was analyzed using different approaches, namely changes of natural population analysis (NPA) charges, Wiberg bond indexes (WBI), and Bader's "atoms in molecule" (AIM) theory (Table 3).

Changes of NPA charges on Al and O atoms appear to be sensitive to the type of complex formed: in DHB complexes the positive charge on Al and negative charge on X become larger, Δq increases with increasing the proton donor strength. In Lewis complexes (**1·M_b** and **1·TFE_b**) charges on Al and O decrease due to the electron donation from the oxygen lone pair, resulting in the Al−O bond formation. Herein, there is a noteworthy difference between

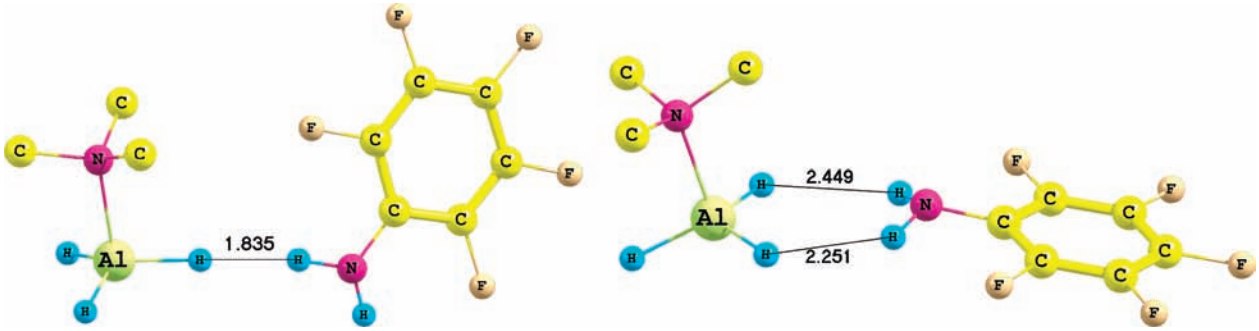

Figure 5. Optimized geometries of DHB complexes of TMAA with perfluoroaniline: monodentate **1·PFA_a** (left) and bidentate **1·PFA_b** (right) (hydrogen atoms of NMe_3 removed for clarity).

DHB and Lewis complexes because upon DHB complex formation the charges on the interacting sites (hydridic hydrogen and XH proton) are always increasing.

The increase of positive charge on the Al atom directly depends on the H···H interaction strength, ranging from 0.023 for PhCCH to 0.087 Å for CF_3OH. The increase of negative charge on the proton donor X atom follows the same trend. The values of electron density on dihydrogen bonds expressed by WBI are also in direct correlation with the H···H bond strength. Bond critical points (3,−1) were found for H···H and Al···O interactions of DHB and Lewis complexes, respectively. The electron densities on critical points (ρ_c) correlate with WBI values. The energies for DHB interactions gathered in Table 3, calculated as the differences between the energy of the complex and the energies of the isolated reactants, also follow the same trend. The energy values range between −1.4 kcal·mol^{-1} for phenylacetylene and −8.2 kcal·mol^{-1} for CF_3OH. WBIs and complexation energies of investigated DHB complexes with neutral aluminum hydrides are significantly smaller than those for related DHB complexes with the anionic aluminum tetrahydride[23] (Table 3). Methanol DHB and Lewis complexation energies are in the same range (−5.6 and −4.8 kcal·mol^{-1}, respectively). On the contrary with TFE, the DHB complex is notably more stable than the Lewis complex (complexation energies of −5.7 and −2.8 kcal·mol^{-1}, respectively). On the whole, computational results confirm the formation of both H···H (DHB) and Lewis (Al−O) complexes of TMAA with alcohols.

IR Spectral and Theoretical Investigations with Bidentate NH_2 Acids. The interaction of TMAA with potentially bidentate NH_2 acids has also been investigated. These polydentate proton donors offer the possibility of two types of coordination when interacting with polyhydrides: the typical monodentate with only one H···H dihydrogen bond and bidentate, entailing interaction of two hydrides with both hydrogen atoms of the XH_2 group and formation of a symmetrical chelated structure, as shown by us previously.[16] Previous calculations of EH_4^-·H_2XR (E = B and Ga) complexes have shown that the preference for monodentate or bidentate structures was dependent on the central atom. This last type of dihydrogen bond was specific to the GaH_4^- anion and was not found for BH_4^-.

In contrast to our previous researches showing that the different coordination types can be attained only by using

Table 4. Calculated Structural, Spectroscopical, and Electronic Characteristics of PFA−TMAA Complexes

	1·PFA_b		
	H···H1	H···H2	**1·PFA_a**[a]
rH···H	2.251	2.449	1.835
∠ NH···H	137.4	129.1	170.0
Δr(NH)	0.003	0.002	0.008
Δr(AlH)^{bond}	0.004	0.003	0.007
Δr(AlH)^{free}	−0.007		−0.005
Δq(Al)	0.013		0.050
Δq(N)[b]	−0.009		−0.005
WBI	0.003	0.001	0.016
ρ_c	0.008	0.006	0.045
ΔE_{ZPVE}	−2.95		−4.05
Δ(NH), cm^{-1}	−38 (−12)		−34 (+42)
(ΔA(NH), km·mol^{-1})	−31 (+144)		−110 (+499)

[a] Data for bonded NH group. [b] N atom in perfluoroaniline molecule.

different proton donors or acceptors, we have found that TMAA is able to form both monodentate and bidentate chelate complexes with perfluoroaniline (PFA) (DFT calculations). Optimization of TMAA−PFA adducts led to two different minima (Figure 5).

The monodentate complex **1·PFA_a** is characterized by geometric parameters similar to those found for other NH acids, such as pyrrole, with practically linear NH···H moiety (Table 4). The NH···H angles in the bidentate complex **1·PFA_b** (137° and 129°) are unfavorable to DHB complexes and smaller than those obtained for symmetrical bidentate GaH_4^- complexes (141−148°).[16] The complex **1·PFA_a** possesses two different weak H···H contacts of 2.251 and 2.449 Å. The last is formally larger than the sum of hydrogens' van der Waals radii, but the elongations of N−H and Al−H bonds suggest the presence of a second H···H interaction. Bidentate coordination was confirmed by electron distribution analysis. For both H···H bonds in the bidentate complex (3,−1) critical points exist, and the presence of an additional ring (3,−3) critical point confirms the formation of the chelate structure. The molecular graph of TMAA−PFA bidentate cycle complex is given in the Supporting Information. Changes in the charges of the Al atom and the proton donor N atom in both complexes follow the same trend as for complexes of monodentate acids (Table 3). WBIs also show the presence of the bond between hydrogen atoms in NH_2^- acid and TMAA hydrides in **1·PFA_b**.

Table 5. Spectroscopic Characteristics of DHB Complexes of Bidentate NH Acids with $(Me_3N)AlH_3$ in Hexane

NH	ν(NH)^{init}, cm^{-1}	ν(NH)^{complex}, cm^{-1}	$\Delta\nu$(NH), cm^{-1}
PFA	3500(as)	3473^{free}	19.5[a,a]
	3407(s)	3291^{bond}	−162.5[a,a]
TeCA	3516(as)	3487^{bond}(as)	−29[b]
	3412(s)	3395^{bond}(s)	−17[b]

[a] $\Delta\nu(NH) = \nu(NH)^{complex} - [\nu(NH)^{as} + \nu(NH)^{s}]/2$. [b] $\Delta\nu(NH) = \nu(NH)^{complex} - \nu(NH)^{init}$.

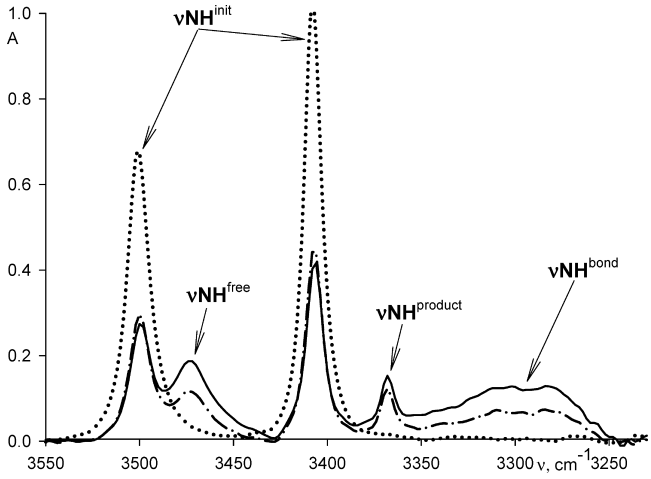

Figure 6. IR spectra in the ν(NH) range of $C_6F_5NH_2$ ($c = 0.01$M) (dotted line) and in the presence of 0.03 M $AlH_3(NMe_3)$ at 190 K (solid line) and at 210 K (dash-dot line) and hexane, $d = 0.22$ cm.

Relative energies of both TMAA−PFA DHB complexes are similar (complexation energies of −4.1 and −3.0 kcal·mol^{-1} for the monodentate and bidentate complexes, respectively), hampering a clear prediction of the experimentally favored complex in solution. In order to benchmark the spectroscopic traces able to discriminate between the two types of dihydrogen bonds, we have followed the same procedure than we used recently in the study of intermolecular vibrations of $H_3EH^-\cdots HOR$ complexes,[31] performing initially a computational study of the vibration spectra. Changes in the N−H frequencies after complexation ($\Delta\nu$(NH)) are collected in Table 5 and will be compared with the experimental frequencies.

Two substituted anilines (perfluoroaniline and 2,3,5,6-tetrachloroaniline) were used experimentally as polydentate acids interacting with TMAA. In the range of the stretching vibrations of NH_2 group of $C_6F_5NH_2$, two bands are observed and assigned to symmetrical (ν^s =3407 cm^{-1}) and asymmetrical (ν^{as} =3500 cm^{-1}) stretching vibrations. In the presence of TMAA, three new bands (3473, 3368, and 3291 cm^{-1}) appear (Figure 6, Table 5). The intensities of two bands (3473and 3291 cm^{-1}) are growing upon cooling while the intensity of the band at 3368 cm^{-1} is not.

Analysis of the data in Table 4 shows that it is possible to recognize the type of coordination of the polydentate proton donor by means of IR spectroscopy. Analysis of the relative width and shifts of these bands helps to determine their character and the type of coordination.

The first new band (ν(NH) = 3473 cm^{-1}) is narrow, but the second band (ν(NH) = 3291 cm^{-1}) is broad, so we suggest that they could be assigned to the free NH and bonded NH···H bonds, respectively. The shift of the bands

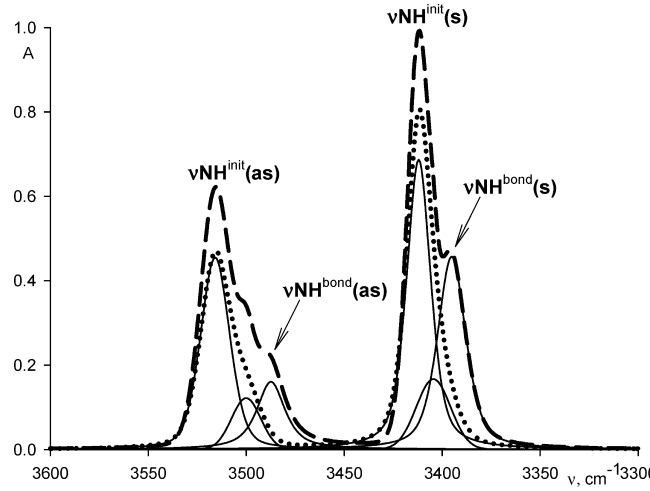

Figure 7. IR spectra in the ν(NH) range of $C_6Cl_4HNH_2$ ($c = 0.01$ M, dotted line) in the presence of 0.025 M $AlH_3(NMe_3)$ (dashed line) with bands of decomposition (solid lines), 230 K, hexane, $d = 0.22$ cm.

relative to their initial positions (3500 and 3407 cm^{-1}) is 27 and 116 cm^{-1}, respectively. These facts are in agreement with DFT results for the monodentate complex and with the spectral pattern for the GaH_4^-−*p*-nitroaniline complex,[16] which was characterized by one H···H bond.

Thus, the new band at 3473 cm^{-1} is attributed to the free NH vibration and the band at 3291 cm^{-1} to the NH···H bonded band. The correct shifts of these bands can be calculated by taking the mean frequency of free PFA $[\nu(NH)^{as} + \nu(NH)^{s}]/2$ as a reference ($\Delta\nu(NH)^{free} = 19.5$ cm^{-1}, $\Delta\nu(NH)^{bond} = -162.5$ cm^{-1}).[16,32]

In the Al−H stretching region, the dihydrogen bond formation leads to the appearance of the low-frequency shoulder ($\nu(AlH)^{bond} = 1678$ cm^{-1} and $\Delta\nu(AlH) = -26$ cm^{-1}) at 190−230 K.

The third band in the ν(NH) region at 3368 cm^{-1} could be assigned to the stretching vibration of one NH group in the PFA where the second NH proton is substituted by $AlH_2(NMe_3)$ (product of one H_2 molecule evolution, see below). The intensity of this band grows upon heating, which is accompanied by a visible gas evolution. At the same time, new high-frequency weak bands at 1815 and 1777 cm^{-1} appear in the Al−H stretching vibration region. These new stretches (one N−H and two Al−H) can be clearly assigned to the product of the aminolysis reaction (eq 2). We suppose a formation of monosubstituted product by analogy with the TMAA−indole system (see above).

$$(Me_3N)AlH_3 + H_2NC_6F_5 \rightleftarrows (Me_3N)H_2AlH\cdots H_2NC_6F_5 \rightarrow (Me_3N)H_2AlNHC_6F_5 + H_2 \quad (2)$$

To support this hypothesis we used NMR spectroscopy. The room-temperature ^{1}H NMR spectrum of $C_6F_5NH_2$ in toluene-d_8 shows a singlet of the NH_2 group at 2.68 ppm. The ^{27}Al NMR spectrum of TMAA in toluene features a broad singlet at 111.6 ppm. The ^{27}Al NMR spectrum of the

(31) Filippov, O. A.; Tsupreva, V. N.; Epstein, L.; Lledós, A.; Shubina, E. *J. Phys. Chem. A* **2008**, *112*, 8198–8204.
(32) Patwari, G. N.; Ebata, T.; Mikami, N. *Chem. Phys.* **2002**, *283*, 193–207.

Table 6. Spectroscopic and Thermodynamic Characteristics of DHB Complexes with $(Me_3N)AlH_3$

HX	P_i	$\Delta\nu$(XH),[a] cm^{-1}	$\Delta H°$,[b] $kcal\cdot mol^{-1}$	$\Delta H°_{calc}$,[c] $kcal\cdot mol^{-1}$
indole	0.75	214	−4.2	−3.4 (pyrrole)
^{i}PrOH	0.63	212	−4.1	−5.6 (methanol)
$C_6F_5NH_2$	0.55	163	−3.3	−3.6[d]
AdCCH	0.26	63	−1.5	−0.5 (phenylacetylene)

[a] $\Delta\nu(XH) = \nu(XH)^{init} - \nu(XH)^{bond}$. [b] From eq 3. [c] DFT calculations. [d] For the monodentate TMAA−PFA complex.

equimolar TMAA−$C_6F_5NH_2$ solution measured immediately after the mixing shows two singlets at 113.4 and 97.4 ppm of a 1:1 integral ratio. The first singlet corresponds to AlH_3NMe_3, and the second singlet corresponds to the reaction product. Correspondingly in the ^{1}H NMR spectrum, the NH_2 resonance shifts to 2.95 ppm (as the result of its involvement in hydrogen bond formation[6a,7a]) and the new singlet appears at 3.05 ppm. The integral intensities ratio of these signals is 2:1. Hence, the changes in IR and NMR spectra allow assigning the new signals to $NMe_3AlH_2NHC_6F_5$.

IR spectra of 2,3,5,6-tetrachloroaniline (TeCA) reveal two bands of NH stretching vibrations $\nu(NH)^{as} = 3516\ cm^{-1}$ and $\nu(NH)^{s} = 3412\ cm^{-1}$, accompanied by weak shoulders at 3499 and 3402 cm^{-1} (Figure 7), which can be assigned to the weak NH−Cl hydrogen bonds of TeCA self-associates. Addition of excess TMAA to the TeCA solution results in the appearance of two new shifted narrow bands at 3487 and 3395 cm^{-1} (Figure 7). The small shifts of these bands ($\Delta\nu(NH)^{as} = -29\ cm^{-1}$ and $\Delta\nu(NH)^{s} = -17\ cm^{-1}$) along with their narrowness are in agreement with the DFT calculation data for a cyclic complex (see Table 4). Thus, we can state the formation of both monodentate and cyclic bidentate complexes by TMAA with different substituted anilines. The cyclic bidentate TMAA−TeCA complex slowly decomposes at room temperature similarly to other complexes studied with formation of a $NMe_3AlH_2NHC_6Cl_4H$ aminolysis product.

Strength of AlH···HX Interaction and TMAA Basicity. The enthalpy of AlH···HX formation ($-\Delta H°$) was determined from the correlation equation:

$$-\Delta H° = \frac{18\Delta\nu}{720 + \Delta\nu} \qquad (3)$$

where $\Delta\nu$ is the shift on the νXH stretching frequency due to dihydrogen bond formation. This equation was proposed by Iogansen for classical H-bonded systems[33−35] and also proved to be applicable for DHB systems. It was shown for numerous DHB complexes of transition-metal,[30] boron, and gallium hydrides[16,12b] with organic acids that the enthalpy values from the eq 3 are in a good agreement with enthalpy values calculated by Vant−Hoff's method. The data in Table 6 show that as in other systems $-\Delta H°$ values of DHB complexes increase with the proton-donor ability of alcohols. As seen from the $-\Delta H°$ values, the AlH−HX hydrogen bonding is of medium strength (4.2−1.5 $kcal\cdot mol^{-1}$).

Calculated dihydrogen bond enthalpies ($\Delta H°_{calc}$) in model systems follow the same trend and have values similar to those estimated from eq 3 (Table 6). The energy of the H···H interaction was estimated using the correlation between the energy of the contact (E_{HH}) and the value of the potential energy density function $V(r)$. The corresponding bond critical point[36] ($E_{HH} = 1/2V(r)$) for CH acid ($E_{HH} = -1.5\ kcal\cdot mol^{-1}$) and NH_2 acid ($E_{HH} = -4.0\ kcal\cdot mol^{-1}$) was in a good agreement with the experiment.

Dependence between $-\Delta H°$ and P_i (proton-donor ability of XH acids) allows one to estimate the proton-accepting ability of the hydride ligand in **1** using the Iogansen's "rule of factors"[33] (eq 4), where P_i is the proton-donating ability for XH acids and $-\Delta H_{11} = 5.7\ kcal\cdot mol^{-1}$ for the standard phenol−diethylether pair in corresponding solvent (hexane) with $P_i = E_j = 1.0$.

$$-\Delta H^{\circ} = -\Delta H_{11} P_i E_j \qquad (4)$$

The basicity factor (E_j) is independent of the proton donor and solvent and characterizes the proton-accepting ability of the H-bonding site. Thus, it is possible to compare the proton-accepting ability of TMAA ($E_j = 1.0 \pm 0.1$) with that of other main-group hydrides in dihydrogen bond formation. TMAA's E_j is significantly greater than that of neutral Et_3NBH_3's hydride ($E_j = 0.53$), but smaller than that of anionic BH_4^- hydride ($E_j = 1.25$).[12b] In spite of this difference between E_j values of TMAA and BH_4^-, the proton-transfer reactions are much more favorable for TMAA in comparison with the BH_4^- anion. Such irregularity was found for protonation of transition-metal hydrides, and this is not rare for such bases.[6]

Proton Transfer Reaction. For most of the alcohols, the experimental detection of reaction intermediates in solution was not possible even at 140 K solely the products were detected. Only in case of the weakest acidic alcohol ^{i}PrOH, the DHB complex can be detected at 190 K by the shift on the ν(AlH) ($\nu(AlH)^{bond} = 1658\ cm^{-1}$, $\Delta\nu(AlH) = 46\ cm^{-1}$) and νOH bands ($\Delta\nu(OH) = 212\ cm^{-1}$). We observe the instant disappearance of initial TMAA and dihydrogen bond ν(AlH) bands when raising the temperature to 200 K. At the same time, the high-frequency bands (1760 and 1790 cm^{-1}) appear, testifying the formation of the monosubstituted product $(Me_3N)AlH_2OCH(CH_3)_2$. Band assignment was made on the basis of frequency calculations. Similar spectral changes were observed studying the interaction between GaH_4^- and OH proton donors.[16] No DHB complex but only protonation product was observed in the IR spectra in the interaction with a stronger alcohol (TFE).

In whole, proton transfer to TMAA from OH acids was observed at a temperature of > 200 K and from NH acids at > 250 K, and only DHB complexes of TMAA with CH acids exist at room temperature without proton transfer (it will be

(33) Iogansen, A. V. *Theor. Experim. Khim.* **1971**, *7*, 302−311; *Chem. Abstr.* **1971**, *75*, 101848.
(34) Iogansen, A. V. *The Hydrogen Bond*; Nauka: Moscow, Russia, 1981, p 134.
(35) Iogansen, A. V. *Spectrochim. Acta, Part A* **1999**, *55*, 1585–1612.
(36) (a) Espinosa, E.; Molins, E.; Lecomte, C. *Chem. Phys. Lett.* **1998**, *285*, 170–173. (b) Espinosa, E.; Alkorta, I.; Rozas, I.; Elguero, J.; Molins, E. *Chem. Phys. Lett.* **2001**, *336*, 457–461.

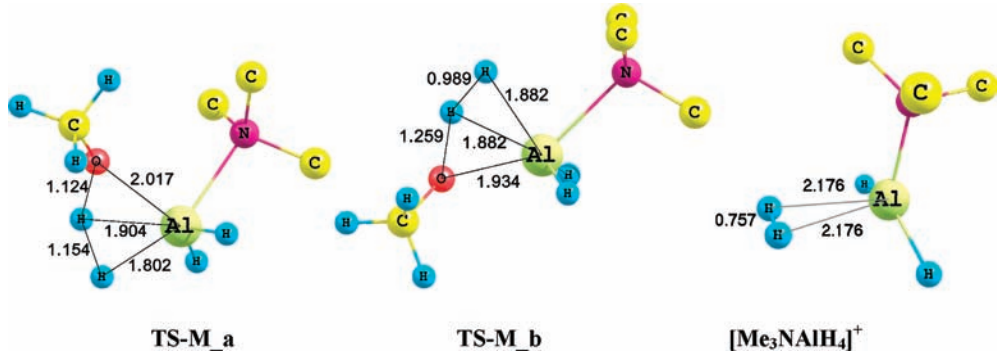

Figure 8. Transition states for proton transfer to TMAA from DHB complex with CH_3OH (**TS-M_a**, left) from the Lewis complex with CH_3OH (**TS-M_b**, center), and the optimized structure of $[Me_3NAlH_4]^+$ (right) (hydrogens of NMe_3 removed for clarity).

observed only in the case of the additionally heated solution). The reaction that is taking place involves nucleophilic attack from the X lone pair and Al−X bond formation accompanied with H_2 formation and release:

$$(Me_3N)AlH_3 + HX \rightarrow (Me_3N)H_2AlX + H_2 \qquad (5)$$

This reaction may play a key role in the formation of stable hydrogen containers, which would be stable at ambient conditions with H_2 evolution occurring only after applying additional actions.

The mechanism of the proton-transfer reaction has been investigated by DFT calculations. The interaction of TMAA with methanol and TFE gives rise to two different adducts (DHB and Lewis complexes, Figure 4), which can be taken as initial intermediates for reaction 5. Two pathways, one (pathway a) starting from the DHB complex (**1·M_a** or **1·TFE_a**) and the second (pathway b) starting from the Lewis complex (**1·M_b** or **1·TFE_b**), have been explored.

Two transition states, one for the dihydrogen bond pathway and the other for the Lewis complex pathway, have been found for the proton transfer with methanol and TFE. Transition state geometries for the reaction with methanol (**TS-M_a** and **TS-M_b**) are depicted in Figure 8. TS structures for the reaction with TFE are similar and can be found in the Supporting Information. Despite the different interaction governing the formation of dihydrogen bond and Lewis intermediates, transition states in pathway b are similar to those in pathway a, and both can be described as dihydrogen complexes. The H_2 and OCH_3 ligands are located in the same manner in both **TS-M_a** and **TS-M_b**, except their relative positions with respect to the NMe_3 ligand: OR is located opposite to this group in **TS-M_a** and adjacent in **TS-M_b**, and the reverse happens for H_2. Obviously this is the result of initial attack position of the alcohol in the intermediates (see Figure 4).

The short H−H distances in the transition states allow describing them as dihydrogen complexes (Figure 8) similar to TSs of proton transfer to AlH_4^-.[23] In order to verify the η^2-H_2 nature of these structures, we have optimized the isolated cation $[(Me_3N)AlH_4]^+$. As for $[AlH_5]$ theoretically characterized as $AlH_3(\eta^2\text{-}H_2)$,[23] the optimized geometry of this cation can be described as $[(Me_3N)AlH_2(\eta^2\text{-}H_2)]^+$ with a H_2 unit weakly interacting with $[(Me_3N)AlH_2]^+$ (Figure 8c). The same arrangement is found in the TSs, the main difference being in the orientation of the η^2-H_2 ligand: while in the pure $Me_3NAlH_4^+$ moiety (Figure 8c) both hydrogens are equidistant to the other hydride ligands (rotation angle is 0°), in TSs the H_2 moiety is rotated (85° in **TS-M_a** and 45° in **TS-TFM**). The shortening of O···Al distances with respect to the intermediate complexes indicates that nucleophilic attack is concomitant with proton transfer. Thus, proton transfer, H_2-elimination, and formation of alkoxo derivatives take place in a single step as it was shown for anionic AlH_4^-.[23] The dual nature of aluminum hydrides having both Lewis acid and basic sites promotes such behavior.

Proton transfer from CF_3OH goes only by pathway a because no Lewis complex was found in this system. The increase of the proton donor strength leads to the transition state (**TS−TFM**), showing a more advanced H−H formation (shorter H−H distance) and a more incipient O−Al attack (longer Al−O distance) (Figure 9). The transition state for proton transfer from NH acid (pyrrole) to TMAA is similar to the**TS-M_a** except there is a weaker N−Al interaction and less advanced H_2 formation.

The relative energies of all the species associated with the reaction profile are presented in Table 7 with the energy of the separated $Me_3NAlH_3 + XH$ taken as a zero of energies. The reaction is strongly exothermic for all the systems with the great energy of stabilization of corresponding organyl oxo- or azo- derivatives playing a main role as a driving force in the proton transfer, as it was for anionic AlH_4^-.[23] Comparing the reaction of CH_3OH with TMAA and AlH_4^-, it can be seen that despite the lower proton-accepting ability and weaker DHB complex of TMAA (ΔE complex = −5.6 and −10.7 kcal·mol^{-1} for TMAA and AlH_4^-, respectively), the energy barrier is considerably lower for TMAA (17.4 kcal·mol^{-1}) than for AlH_4^- (27.3 kcal·mol^{-1}). Comparing the geometries of both transition states, this decrease can be attributed to the stronger Al−O interaction in the TMAA system. Although most of the distances are similar in both TSs, the Al−O is considerably shorter for TMAA (2.017 Å) than for AlH_4^- (2.232 Å).[23] Whereas proton transfer is easy for the anionic hydride, nucleophilic attack is favored in the neutral hydride, resulting in an energy barrier decrease. The TMAA alkoxo product is also more stable (−27.5 and −24.0 kcal/mol, respectively, Table 7). Pathway b from the Lewis complex has a somewhat lower barrier (14.3 kcal·mol^{-1}) and leads to the same product. The same trends

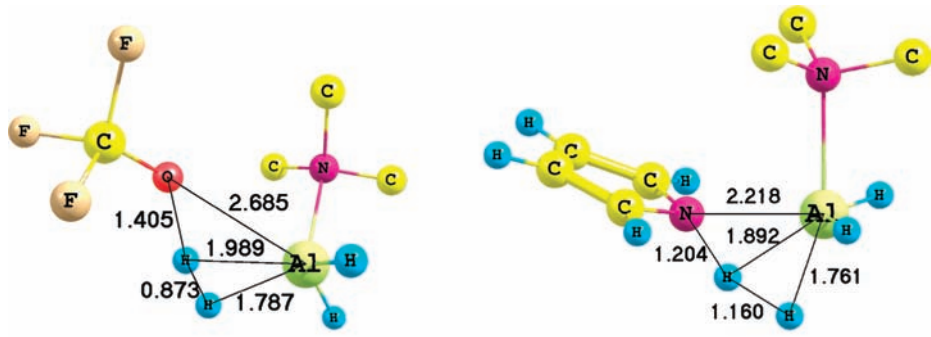

TS-TFM TS-pyrr

Figure 9. Transition states for proton transfer to TMAA from CF_3OH (**TS−TFM**) and from pyrrole (**TS−Pyrr**) (hydrogen atoms of NMe_3 removed for clarity).

Table 7. Relative Energies (in kcal·mol^{-1}) for Complexes, TSs, and Products of the Reaction of Aluminum Hydrides with Proton Donors[a]

type of complex	ΔE complex[b]	ΔE TS[b]	ΔE product[b]	$\Delta E^{\#c}$
TMAA−CH_3OH (pathway a)	−5.6	11.8	−27.5	17.4
AlH_4^-−*CH_3OH*[d]	*−10.7*	*16.6*	*−24.0*	*27.3*
TMAA−CH_3OH (pathway b)	**−4.8**	**9.5**	**−27.5**	**14.3**
TMAA−TFE (pathway a)	−5.7	12.9	−30.8	18.6
AlH_4^-−TFE[d]	*−17.0*	*5.5*	*−33.8*	*22.5*
TMAA−TFE (pathway b)	**−2.8**	**9.0**	**−30.8**	**11.8**
TMAA−CF_3OH	−8.2	7.6	−38.7	15.8
AlH_4^-−CF_3OH[d]	*−21.8*	*−16.5*	*−48.1*	*5.3*
TMAA−Pyrrole	−3.4	26.6	−19.2	30.0
TMAA−$(CH_3OH)_2$ (via **1·2M_a**)	−13.0	6.6	−35.6	19.6
TMAA−$(CH_3OH)_2$ (via **1·2M_b**)	**−14.3**	**−2.0**	**−35.6**	**12.3**

[a] ΔE are the electronic energies, including zero-point vibrational correction. [b] The energy of separated $R_3AlH + XH$ is taken as a zero of energies. [c] Energy barriers (energy of TS respective to the corresponding complex). [d] From ref 23.

are found for the reaction with TFE: pathway b barrier (11.8 kcal·mol^{-1}) is lower than pathway a (18.6 kcal·mol^{-1}), and both are lower than that for AlH_4^- (22.5 kcal·mol^{-1}). On the contrary for CF_3OH, the barrier for AlH_4^- (5.3 kcal·mol^{-1}) is considerably lower than that for TMAA (15.8 kcal·mol^{-1}), proving that this reaction is governed by the basic strength of the hydride proton acceptor. Calculated energetic characteristics of the proton transfer from pyrrole to TMAA explain different behavior of OH and NH acids in the experiment. Namely, the higher transition-state energy in the case of pyrrole can explain the observation of the proton-transfer process only at higher temperatures in comparison to OH proton donors.

It has been shown that proton-transfer reactions with weak Brønsted acids as alcohols are favored by the presence of a considerable excess of alcohol.[37] A key factor for explaining this fact is the stabilization of the alkoxide anion product by strong H-bonding with the excess of alcohol, forming $[RO\cdots HOR]^-$ homoconjugate pairs.[7b,31] Although in our systems the alkoxide anion is bonded to the aluminum in the products, we have also studied the possibility of cooperative effects by including in the calculations a second alcohol molecule.[38] Two possibilities have been considered for the initial placement of this additional CH_3OH molecule: (a) solvating only the first methanol molecule and (b) interacting also with the hydride. The second possibility arises from computational evidence of solvent assistance in proton-transfer reactions in systems containing both donor and acceptor sites with solvent molecules acting as bifunctional catalysts.[39] In particular, it has been reported that ethanol molecules can play such a role.[40]

Optimization of the TMAA−$(CH_3OH)_2$ systems affords the two complexes depicted in Figure 10. When the second CH_3OH molecule is only interacting with the first one, as in a normal methanol dimer situation (**1·2M_a**, Figure 10a), strengthening of the DHB complex occurs (H···H distance shortens by 0.071 Å and interaction energy increases by 7.4 kcal·mol^{-1}). Although the increase in the interaction energy is mainly due to the additional R−OH···OHR hydrogen bond, there is also a cooperative effect. Energetically the cooperative effect can be expressed as $\Delta E_{coop} = \{\Delta E(\mathbf{1\cdot 2M\_a}) - [\Delta E(\mathbf{1\cdot M\_a}) + \Delta E(CH_3OH\cdots OHCH_3)]\}$, and its value $\Delta E_{coop} = -1.6$ kcal·mol^{-1} is lower than that obtained for the stronger ruthenium dihydride $(PP_3)RuH_2$ ($E_j = 1.33$).[41] In addition to the traditional structure of a H-bond complex with a methanol dimer, a second minimum was found with the formation of a six-membered ring via three new bonds (classical H-bonding between methanol molecules, dihydrogen bond OH···HAl and Lewis interaction Al−O) (**1·2M_b**, Figure 10b). Formation of this ring complex is energetically more favorable than **1·2M_a** by 1.3 kcal·mol^{-1}, cooperative effect doubling from **1·2M_a** to **1·2M_b** (Table 7). Namely both types of complexes can be intermediates of proton transfer from weak OH acids to TMAA in the presence of an alcohol excess. Alcoholysis reaction starting from both intermediates has been explored.

(37) Belkova, N. V.; Besora, M.; Epstein, L. M.; Lledós, A.; Maseras, F.; Shubina, E. S. *J. Am. Chem. Soc.* **2003**, *125*, 7715–7725.

(38) (a) Jeffrey, G. A.; Saender, W. *Hydrogen Bonding in Biological Structures*; Springer-Verlag: Berlin, Germany, 1991, chapter 2.6. (b) Karpfen, A. *Adv. Chem. Phys.* **2002**, *123*, 469–510.

(39) (a) Lledós, A.; Bertrán, J. *Tetrahedron Lett.* **1981**, *22*, 775–778. (b) Bergquist, C.; Bridgewater, B. M.; Harlan, C. J.; Norton, J. R.; Friesner, R. A.; Parkin, G. *J. Am. Chem. Soc.* **2000**, *122*, 10581. (c) Prabhakar, R.; Blomberg, M. R. A.; Siegbahn, P. E. M. *Theor. Chem. Acc.* **2000**, *104*, 461–464. (d) Jee, J.-E.; Comas-Vives, A.; Dinoi, C.; Ujaque, G.; van Eldik, R.; Lledós, A.; Poli, R. *Inorg. Chem.* **2007**, *46*, 4103–4113.

(40) Comas-Vives, A.; González-Arellano, C.; Corma, A.; Iglesias, M.; Sánchez, F.; Ujaque, G. *J. Am. Chem. Soc.* **2006**, *128*, 4756–4765.

(41) Gutsul, E. I.; Belkova, N. V.; Sverdlov, M. S.; Epstein, L. M.; Shubina, E. S.; Bakhmutov, V. I.; Gribanova, T. N.; Minyaev, R. M.; Bianchini, C.; Peruzzini, M.; Zanobini, F. *Chem. Eur. J.* **2003**, *9*, 2219–2228.

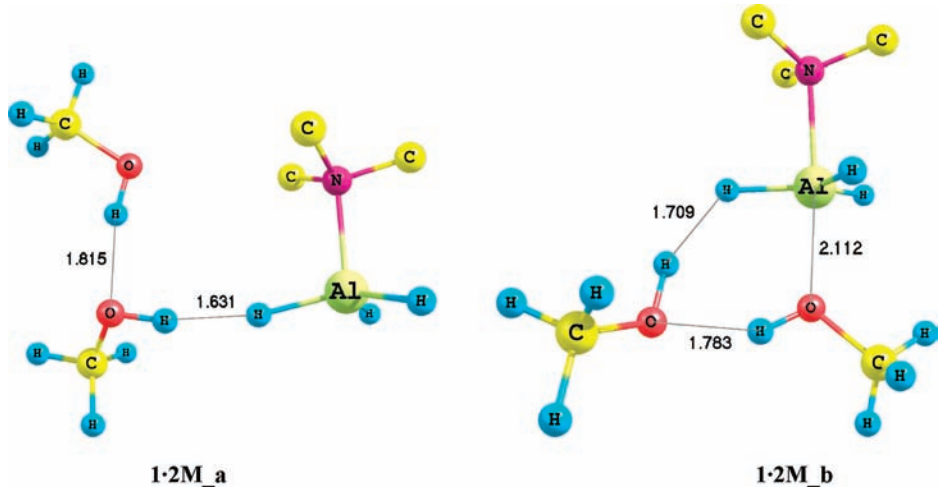

Figure 10. Complexes of TMAA with two methanol molecules: cooperative DHB complex **1·2M_a** (left) and ring complex **1·2M_b** (right) (hydrogens of NMe_3 removed for clarity).

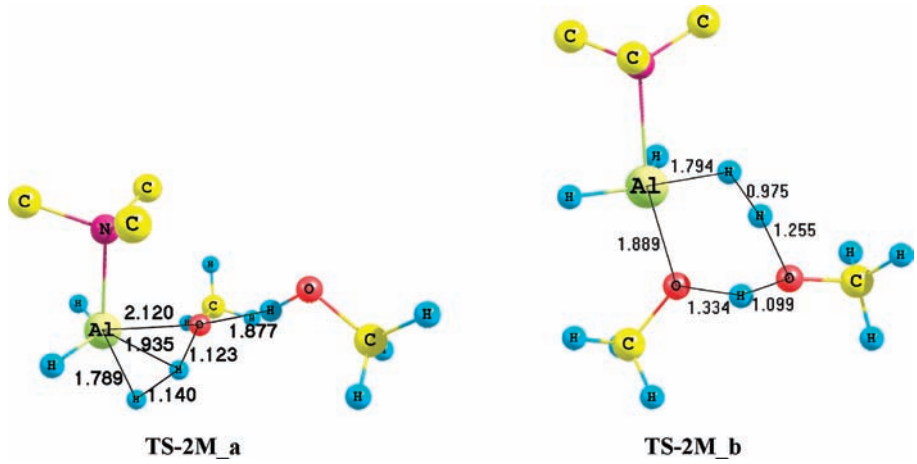

Figure 11. Transitions state for proton transfer to TMAA involving two CH_3OH molecules: **TS-2M_a** from cooperative DHB complex (left) and **TS-2M_b** from ring complex (right) (hydrogens of NMe_3 removed for clarity).

While proton transfer from methanol in **1·2M_a** proceeds (through transition state **TS-2M_a**, Figure 11a) in the same way as to **1·M_a**, starting from the ring complex **1·2M_b** the proton is transferred by a different way: the new Al−O bond is formed with the ROH molecule initially interacting with the Al atom, while a proton from the initially dihydrogen bond CH_3OH molecule goes to the hydride to form the dihydrogen molecule. The second methanol molecule is acting as a bifunctional catalyst, transferring a proton to the hydride and accepting a proton from the Al-bonded methanol molecule. All of these phenomena take place in one step through a six-membered transition state (**TS_2M_b**, Figure 11b). Whereas the energy barrier associated with the first type of solvent assistance in **TS-2M_a** is slightly higher than in **TS-1_a** (19.6 and 17.4 kcal·mol^{-1}, respectively), the barrier in the six-membered ring mechanism is notably reduced (12.3 kcal·mol^{-1}). Participation of the second CH_3OH molecule also favors the exothermicity of the reaction, product stabilization energy increasing by 8.1 kcal·mol^{-1}.

Conclusions

It has been shown from variable-temperature IR investigation that TMAA forms DHB AlH−HX complexes (X = C, N, and O) in solution with a number of XH acids. The spectroscopic features, strength and TMAA basicity factor (E_j), structural parameters, as well as electronic and energetic characteristics of these complexes were determined by combining experimental and theoretical approaches. The existence of both monodentate and bidentate chelate complexes of TMAA with bidentate NH_2 acids was disclosed the first time in solution. The complex with typical monodentate coordination was experimentally found in the system TMAA−PFA, whereas in the system TMAA−TeCA the complex with bidentate coordination was spectroscopically characterized. DHB complexes are intermediates in the proton-transfer reaction, which entails formation of an Al−X bond and H_2-elimination. The extent of this reaction is very dependent on the acid strength: proton transfer to TMAA from OH acids was observed at temperature >200 K and from NH acids >250 K, and only DHB complexes of TMAA

with CH acids exist at room temperature without proton transfer. The reaction that is taking place involves, in addition to the proton transfer, nucleophilic attack from the X lone pair to the Al center. We have found that the dual acid−base nature of neutral aluminum hydrides having both a Lewis acid site (Al) and a basic site (hydrides) allows, besides the dihydrogen bond pathway for proton transfer, another pathway starting from a Lewis complex to be at work. Preference for one of the pathways is related to the acid strength and nucleophilicity of the proton donor. Increasing of OH acid proton-donating ability results in proton transfer via the dihydrogen bond intermediate. Calculations have shown that increasing the proton-donor concentration allows the reaction to take place with a new mechanism, starting from a six-membered intermediate with a second R−OH molecule interacting with both a hydride and the first R−OH molecule. The second molecule acts as bifunctional catalyst accepting and transferring a proton and decreasing the energy barrier. This result points out that these types of complexes, involving two proton donor molecules, could be intermediates of a proton transfer from weak OH acids to the TMAA in the presence of an excess of proton donor. In conclusion, the combined experimental and theoretical study of TMAA complexes with weak proton donors allows understanding the mechanism of proton-transfer and H_2-elimination reactions of aluminum hydride and gives some hints on the factors that could control proton transfer to neutral aluminum hydrides in solution.

Acknowledgment. This work was supported by the Russian Foundation for Basic Research (No. 07-03-00739), Russian Federation President Grant (MK-380.2008.3), INTAS YSF (06-1000014-5809), and Spanish MICINN (Project CTQ2008-06866-C02-01/BQU). The use of the computational facilities of the Centre de Supercomputació de Catalunya is greatly appreciated.

Supporting Information Available: Tables of optimized geometries (Cartesian coordinates) for all the calculated species and the molecular graph of TMMA−PFA bidentate cycle complex. This material is available free of charge via the Internet at http://pubs.acs.org.

IC802262H